X International Conference on Computational Methods in Marine Engineering
MARINE 2023
J. Garcia-Espinosa, L. González, J.E. Gutiérrez & B. Serván-Camas (Editors)

Influence of windsurfing fin stiffness distribution on the lift-drag characteristics

MARINE 2023

Hanna Pruszko* [1], Maciej Reichel [1, 2] and Tomasz Mikulski[1]

[1] Gdańsk University of Technology, Faculty of Mechanical Engineering and Ship Technology, ul. Gabriela Narutowiczan11/12, 80-233 Gdańsk, Poland, web: https://wimio.pg.edu.pl/en/homepage

[2] Prof. Lech Kobyliński Foundation for Safety of Navigation, 14-200 Iława - Kamionka, Poland, web: https://www.ilawashiphandling.com.pl

* Corresponding author: Hanna Pruszko, hanna.pruszko1@pg.edu.pl

ABSTRACT

This article addresses the problem of determining the hydromechanical loads generated by flexible hydrofoils. The research was done on the example of the composite windsurfing fin for the RS:X monotype class. Despite the assumption of fins identity, everyday practice showed that variations of mechanical properties occur and strongly affect their performance. Therefore, we decided to study the differences between the windsurfing fins' stiffness and quantify the resulting variations in performance. The study was done using mainly computational methods supported by the experimental investigation. The two-way Fluid-Structure Interaction (FSI) calculations were performed to investigate this problem. From a large population of measured fins, three fins were selected for calculations, each representing various stiffness properties – rigid, moderate and flexible.

The FSI calculations were performed using Abaqus and Star-CCM+ explicit coupling. The substitute Finite Element Method (FEA) model was created since the composite stacking sequence was unknown. Each fin was divided into eight sections, and the material properties of each section were identified based on the experimental investigation results. The FSI calculations aimed to find lift and drag forces generated by the fins with various stiffness distributions and the quasi-static deformation of the structure. The calculations were performed for one speed and several angles of attack. Based on that, the lift and drag forces were evaluated. The calculations obtained for flexible fins were compared to a rigid hydrofoil. Significant differences between the performance of the fins were obtained, depending on the hydrofoil angle of attack.

Keywords: STAR CCM+; Abaqus; FEA; CFD; RS-X.

NOMENCLATURE

Et	Shell bending stiffness [N/m]
E	Young Modulus [Pa]
w	State variable - displacement [m]
t	Plate thickness [mm]
$\delta\mathbf{x}$	variable vector variations [-]
CFD	Computational Fluid Dynamics
FEM	Finite Element Method
FSI	Fluid Structure Interaction

1. INTRODUCTION

The rapid development of composite materials has resulted in their application in multiple engineering structures. The advantages are light mass, high weight-related strength, corrosion resistance, and design flexibility (Navagally 2017). Apart from aerospace and wind turbine industries, composites are widely used in civil engineering applications, for example, the construction of pedestrian bridges (Chróścielewski et al. 2019; Ferenc and Mikulski 2020a). The known advantages explain why this material plays such a key role in high-performance sailing, for example, as with hydrofoil manufacturing.

In many studies, a strong focus was put on assessing the problem of the relation between the lay-up of composite material and its deformation resulting in variation of hydromechanical characteristics. Boyd et al. (2015) performed one-way FSI computations by obtaining a pressure field from CFD software and applying it to the FEA software. The orientation of plies inside the structural software was modified to check the response of the hydrofoil. It was proved that obtaining the desired deformation by adequately tailoring the material is possible; however, strong coupling is necessary to capture the deformation. Therefore, the Fluid-Structure Interaction methods find an application in optimising and analysing various sailing appendages and rigid sails.

The idea of tailoring the hydrofoil performance was used to design a Passive Adaptive Composite structure for moth foil (Marimon Giovannetti et al. 2018; Marimon Giovannetti 2017). Sacher et al. (2018) performed the optimisation of the hydrofoil for the 35th America's Cup high speed racing yacht. The FSI method was also used to optimise appendages of high-speed racing yacht (Balze et al. 2017). The 3D lifting line theory was coupled with the modified beam method to optimise the mass and stiffness of the America's Cup flying catamaran daggerboard. Sacher et al. (2020) used the coupling of the Abaqus software with a lifting line–based flow model to calculate the forces and deformations of semi-rigid yacht sails. Ponte, Sutherland, and Garbatov (2022), based on the information from the moth sail yacht producers manufactured and built the FEA model of the main strut for further FSI testing. They found good agreement between the Abaqus FEA model and experimental results.

There are few works focusing on the problems of Fluid-Structure Interaction for windsurfing fins so far (Sutherland et al. 2022) and (Cardoso de Brito et al. 2022) investigated the hydroelastic performance of the commercial windsurfing fin and performed two-way FSI analysis of the influence of ply orientation on the tip twist. The object of study was a slalom fin with a 0.37 m span analysed for a range of speed from 10 knots to 35 knots and from 2 degrees to 6 degrees angle of attack.

This article addresses the problem of assessing the hydro-structural properties of composite windsurfing fins employing Fluid-Structure Interaction calculations. The research subject is the windsurfing fin for ex-Olympic class RS:X. Despite the assumption of fins identity, everyday practice showed that variations of mechanical properties occur and strongly affect their performance. Therefore, we decided to study the differences between the windsurfing fins' stiffness and quantify the resulting variations in performance, which is the main objective of the presented research. Both experimental and numerical methods were used for this purpose.

The main challenge of this research was to create a substitute hydroelastic model of the hydrofoil. In this case, direct modelling of the composite was not possible due to a lack of detailed information about the laminate fabrication – material, lay-up and manufacturing details. Current state-of-the-art proves that we are able to predict the hydroelastic properties of the objects if we possess all the necessary data regarding the shape, composite lay-up and production process details. However, from the end-user point of view, these data are simply unavailable, and hydroelastic modelling using reverse engineering methods is almost not addressed at all. So far, only one work focused on numerical investigation of the hydroelastic properties of the hydrofoil with a completely unknown internal structure. Marimon Giovannetti et al. (2022) performed the experiments to evaluate the performance and deformation of the NACRA 17 hydrofoil in the cavitation tunnel for different combinations of water speed, leeway and rake angles. The FSI calculations were also performed, finding good agreement with drag and lift forces; however, some discrepancies were found for the twist angles.

Our current work presents an alternative approach to model the hydroelastic properties of the composite material. The evaluated methodology is used to assess the range of variances in deformation under the fluid loading, lift and drag forces for three selected windsurfing fins.

The remaining part of the article is organised as follows: Section 2 presents materials and methods, including the research object, the methodology of generation and verification of the Finite Element Method model, and the numerical setup for the FSI simulations. Section 3 presents the results of the numerical investigation, followed by a discussion in Section 4 and conclusions in Section 5.

2. MATERIALS & METHODS

2.1 Research object

The subject of the research is the windsurfing fin for the monotype racing board RS:X. It is a monotype class, which has two implications. Theoretically, all the fins should be the same; however, the differences in the performance are felt by the windsurfers themselves. Additionally, the internal lay-up, materials, and manufacturing details are the producer's intellectual property, and they are unknown to us.

Above a given speed of the board, the fin is the only control surface responsible for generating the side force that allows keeping the course of the board – Figure 1. This hydrodynamic side force balances the aerodynamic sail force but simultaneously results in bend-twist deformation of the fin. However, the range of deformations is unknown, as well as the variance in hydroelastic properties for various fins.

The span of the fin for male competitors is equal to 0.66 m, and the chord next to the head is equal to 0.13 m. The fin planform shape resembles an ellipse, but it has not pure elliptic shape. The aspect ratio of the fin is equal to 6.84, and the planform area is equal to 0.06175 m^2. The exact 3D geometry of the fin was created using reverse engineering tools. The model was scanned using the 3D scanner, and the obtained a cloud of points was faired. Later on, the cross sections were generated and used for obtaining the final geometry of the fin. Details of this process and assessment of the hydrodynamic loads were presented by (Pruszko 2021).

Figure 1. The RS:X fin

2.2 Finite Element Method Model

In this article, we propose an approach in which a composite structure is modelled as an isotropic material. The calculations that included such simplification were presented by (Kreja and Sabik 2019). The optimisation of the sandwich composite footbridge with a U-shaped cross-section modelled parts of the bridge as an isotropic material was found (Ferenc and Mikulski 2020b). This simplification proved its usefulness; therefore, it was used for this study as well.

The composite was modelled as a core represented by solid 3D elements, and the outer layer of the laminate was modelled as a shell. Because of problematic geometry features, i.e., leading and trailing edges, the core was modelled using 3D solid tetrahedral 10-noded elements. Triangular and quadratic 2D shell elements represented the skin. The 3D solid tetrahedral 10-noded elements were generated using existing nodes of 2D shell elements. The nodes' coincidence was checked, and coincident nodes were merged. As a result, all shell elements nodes were common with the 3D solid tetrahedral nodes. Such an approach could also be found in (Chróścielewski et al. 2019; Ferenc and Mikulski 2020a). The thickness of the plate property was assessed based on the measurements of fin sections. A similar approach was proposed by (Maung et al. 2021); however, the outer laminate was modelled as a hexahedral solid element. The total count of the elements was equal to 22705 and included 76 triangular elements, 4147 quadratic elements, and 18482 tetrahedral 10-noded elements. The model had 33084 nodes. The mesh is presented in Figure 2.

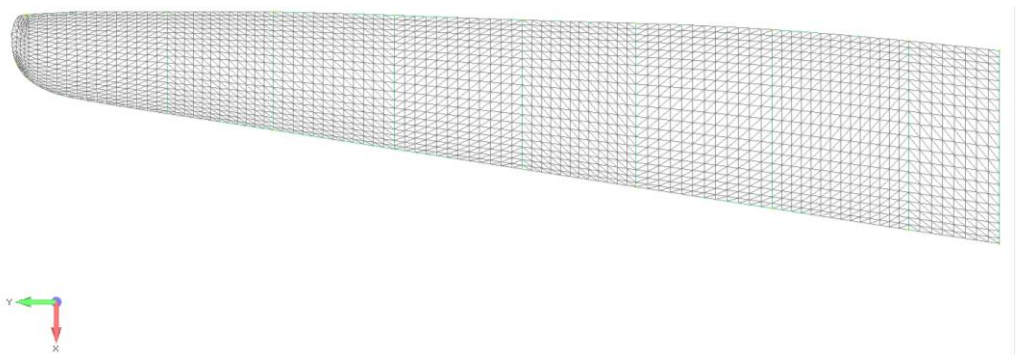

Figure 2. The FEM mesh

To obtain validation data, experiments on a large number of fins were carried out. From the entire population, three fins were selected for validation. The first represented the flexible structure, the second stiff structure, and the third moderate. The fin was rigidly clamped by its head during the experiment and loaded with a force equal to 130 N at a distance of 0.6 m from the fin head. A laser rangefinder measured the displacements at three different points (Figure 3).

The boundary condition, load, and control points were applied in the FEA model - schematically presented in Figure 3. The fixed boundary conditions were applied for the fin's top cross-section to represent the experimental conditions. The model was devided into eight sections to correctly represent varying bending stiffness along the fin length.

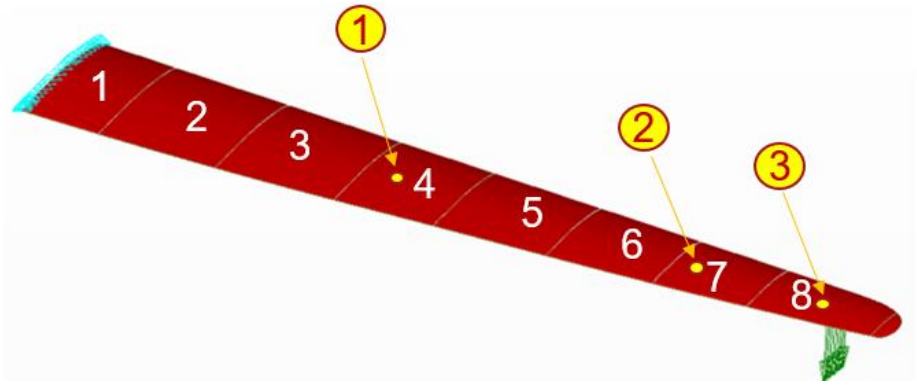

Figure 3. Boundary conditions and loads

The quantity responsible for higher or lower susceptibility for deformations is the global bending stiffness EI_y. which can be expressed as in Eq. 1:

$$EI_y = \int_0^{s_1} E\frac{1}{2}h^2(s)tds = Et\left[\frac{1}{2}\int_0^{s_1} h^2(s)\,ds\right] \tag{1}$$

Where *Et* [N/m] is the membrane shell stiffness, h [m] is the distance from the elemental cross section to the neutral axis, and s is the local coordinate alonde the cross section contour, this is schematically presented in Figure 4.

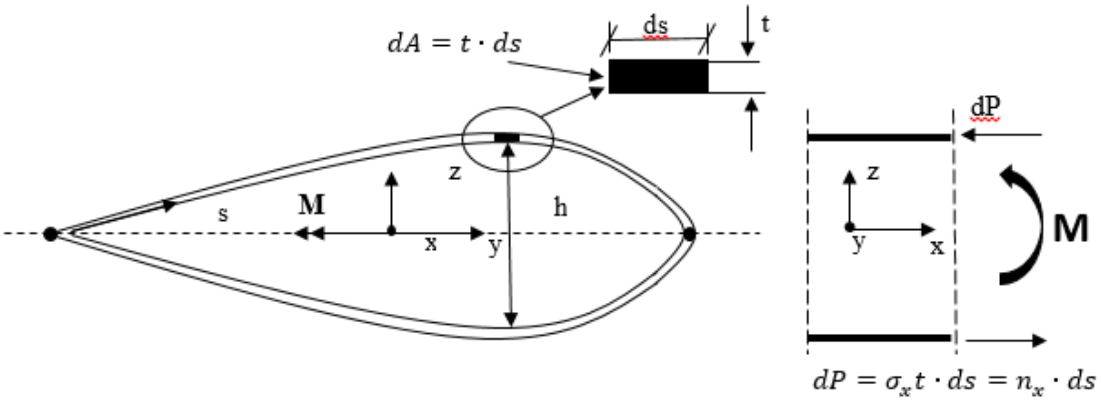

Figure 4. The bending stiffness

It can be noticed that any changes to the membrane shell stiffness can be realized by modifications of the Young Modulus *E* or shell thickness *t*, according to the Eq. 2:

$$\delta EI_y = \delta(Et)\left[\frac{1}{2}\int_0^{s_1} h^2(s)\,ds\right] \tag{2}$$

Therefore, the variations in the membrane bending stiffness can be written as follows in Eq. 3:

$$\delta(Et) = E\cdot\delta t \;\; or \;\; \delta(Et) = \delta E\cdot t \tag{3}$$

It was decided that only the stiffness of the outer layer would be identified, whereas the core has the constant value of Young Modulus along the entire length of the fin. For the stiffest fin, the plate thickness was assumed to be equal to 0.002 m; for medium, it was equal to 0.0018 m; for most flexible, it was equal to 0.0015 m. Therefore, the only variable – the state parameter varying for each section and every fin - was the Young Modulus. Therefore, the variations of plate membrane stiffness were realized through modification of plate Young Modulus, according to Eq. 4:

$$\mathrm{E} \;=\; \mathrm{const} \;\Rightarrow \delta EI_y \;\rightarrow \delta E \tag{4}$$

In general, the model can be described by constant parameters and design variable vector **x**. In this case, the identified parameters were the Young Modulus of fin sections for $\mathbf{x_j}$, j = 1,2,..,8, so the correct values of model parameters need to be derived. They can be evaluated and validated by comparing the measured state variable $\widehat{w}_i$ with state variables obtained numerically w_i for i = 1,2,3. The measured variable $\widehat{w}_i$ was the displacement in the control point *i*, and s_i was the displacement in the control point *i* assessed with FEA calculations. The optimisation procedure based on the sum of the least square method described below was applied for the problem of validation and identification of each section's stiffness properties. The identification problem was formulated as follows:

$$\min F(\delta \mathbf{x}) = \sum_{i=1}^{3} [\,(w_i + \delta w_i) - \widehat{w}_i]^2 \tag{5}$$

Where $\delta w_i(\delta \mathbf{x})$ – is the state variable variation due to design variable vector **x** variations**,** namely, the variations of the displacement in the i-th control point due to the variations of the Young Modulus of fin sections.

The first-order sensitivity method was used to solve the identification problem. In structural mechanics, sensitivity analysis focuses on evaluating the direct dependency between structure response variation due to variation of design variables. If the design variables form a set of numbers, the state variable is described by the characteristic function $w(\mathbf{x})$, where **x** is a vector of design variables. In most problems, we do not know the direct relationship between the state variable function $w(\mathbf{x})$ and design variables **x.**

The MATLAB optimisation toolbox was used to solve the optimisation problem defined in Eq. (5) and evaluate the components of the design variable vector $\delta \mathbf{x}$ of the objective function. The least-square linear solver with the interior-point algorithm was used to find the minimum of the expression. The optimisation problem could be classified as searching the function minimum without constraints. The presented issue is not a typical optimisation problem; however, we use the optimisation tool to find the components of design variable vector variations on each step of the identification problem. It allowed us to obtain the target Young Modulus values for each section.

The identification procedure was done in FEMAP. For FSI calculations, the model was imported to ABAQUS and checked for confirmation of the results. Using the SIMULIA co-simulation engine, the structural solver was coupled with STAR-CCM+.

2.3 Fluid-Structure Interaction setup

Three fins with identified stiffness distributions were used for FSI calculations. The CFD solver was already checked and compared; the results of the CFD calculations of the rigid windsurfing fin were presented by (Pruszko 2021). The flow was modelled as a single-phase, turbulent, viscous and incompressible with k-ω SST turbulence model and wall functions. The calculations were performed for three angles of attacks equal to two, four, and six degrees. Fluid forces – namely lift and drag, and structure displacement, were assessed for the water velocity equal to 10 m/s.

According to the ITTC guidelines (ITTC 2011), if a significant lift force is generated by the lifting surface, then the upstream boundary plane should be placed at least 10 chord lengths in front of the body and the downstream boundary 20 chord lengths behind it. This rule was used for the simulations, so the domain length was equal to 6 meters. Side boundaries were placed 1 meter from the fin. The top boundary overlapped the fin's head, and the bottom boundary was placed 1 meter below the tip. For the upstream, the velocity inlet condition was selected. The downstream boundary had assigned the pressure outlet condition. The symmetry condition was assigned to the bottom and side boundaries. The top boundary was a slip-wall. The summary of the boundary conditions is presented in Figure 5.

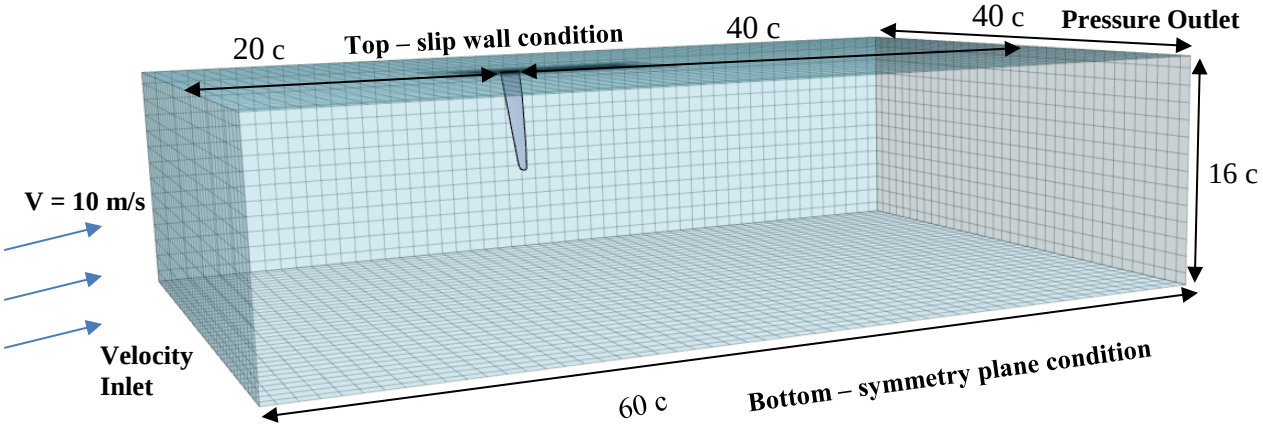

Figure 5. The FSI calculation domain

The mesh resolution had to be high enough to accurately represent the geometry, especially leading and trailing edges, and capture all the flow's relevant features. On the other hand, it should not be too expensive. Mesh refinements were applied on the tip and nose of the fin, in close proximity to the model and the wake region, including the expected area of tip vortex generation. The mesh coarsening was applied on the outside domain boundaries, where a high number of cells is unnecessary. A systematic study of the influence of the mesh base size was performed, resulting in mesh cell counts equal to 1.2 M cells, 2.6 M cells and 5.7 M cells. Little differences were found in the values of displacement and forces, and the medium mesh was selected as a compromise between the accuracy and computation time resources. There were eight prism layers with a maximum thickness of 0.002 m and prism layer stretching equal to 1.3. The values of y+ were slightly above 30. The numerical mesh used to evaluate the hydroelastic properties of the windsurfing fin is presented in Figure 6.

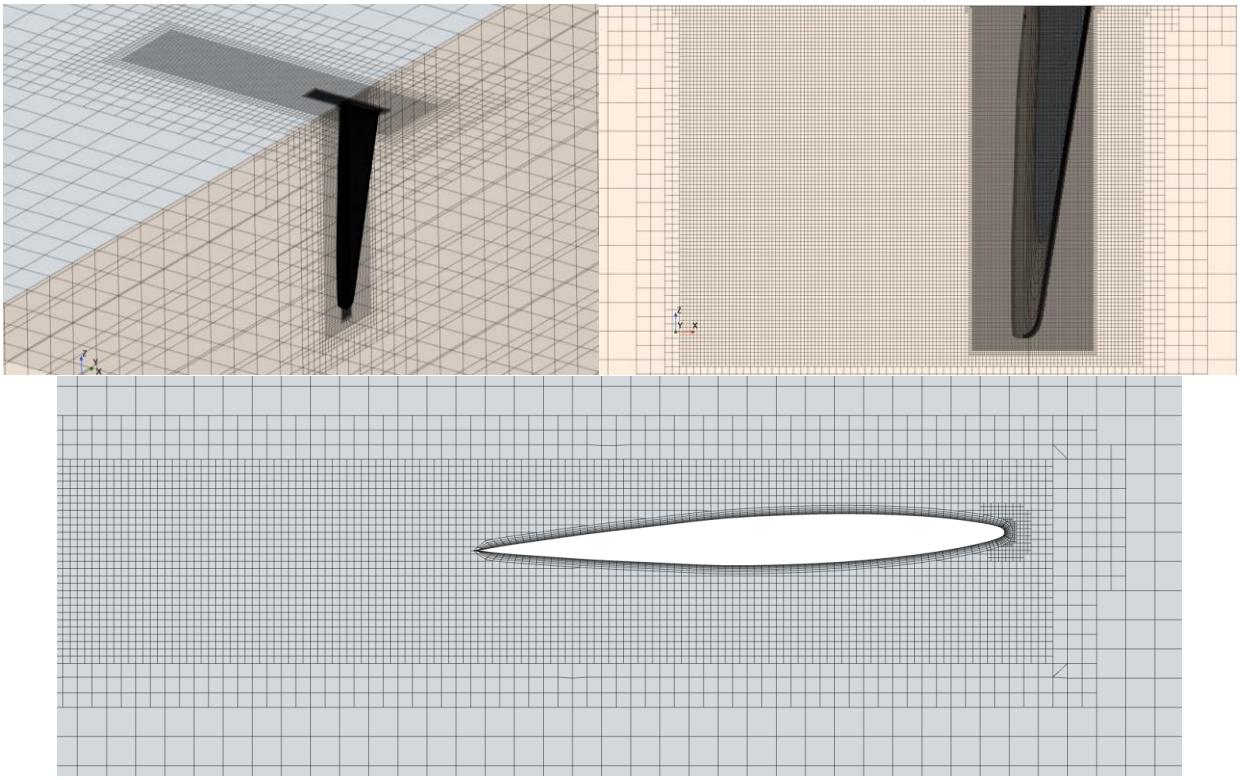

Figure 6. Fluid numerical mesh

The systematic time step sensitivity study for three time steps: 0.001 s, 0.002 s, and 0.004 s showed that the time step of 0.004 s was sufficiently small. The second order implicit solver was applied and explicit coupling using the Gaus-Seidel scheme was selected. The exchange of information regarding the deformation of the structure and new pressure field was done once a time step.

3. RESULTS

3.1 Finite Element Method Results

The results of the static load experiment are presented in Figure 7 in the form of displacement lines. Even for moderate loading equal to 130 N of concentrated force, the displacement of the tip can vary from 0.048 m to 0.067 m. At the first control point, the displacement varied between 0.012 m and 0.017 m. The displacement measured in the second control point was between 0.047 m and 0.032 m.

The identification study with the first-order sensitivity study allowed us to calibrate the values of plate Young Modulus for each section to a very satisfactory level. The difference between the numerical and experimental values did not exceed 1.5 %, and on average, it was equal to 0.54 %. Therefore, the process of identification has a very high accuracy.

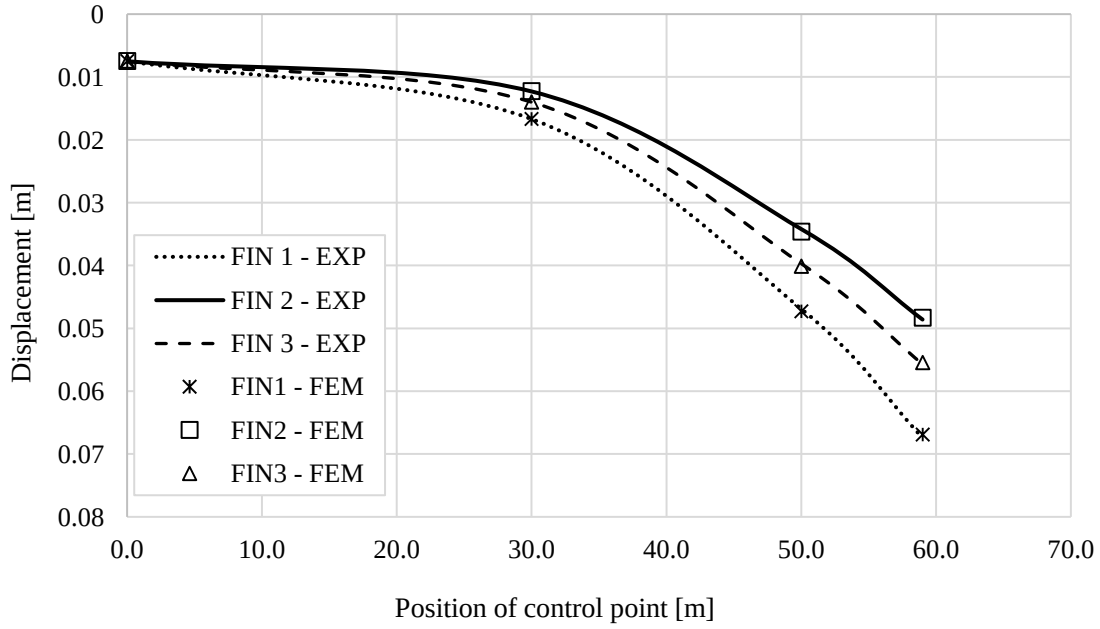

Figure 7. Numerical and experimental results – the displacements in the control points

The final values of identified plate bending stiffness for each fin and every section are presented in Table 1. It can be noticed that significant differences occur, and it is expected that it will have a reflection in the displacement under fluid loading and influence the hydrodynamic forces generated on hydrofoils.

Table 1. Values of bending stiffness of each section [N/m]

	Et_1	Et_2	Et_3	Et_4	Et_5	Et_6	Et_7	Et_8
FIN1	$3.59 \cdot 10^6$	$5.01 \cdot 10^6$	$5.24 \cdot 10^6$	$5.26 \cdot 10^6$	$3.94 \cdot 10^6$	$2.71 \cdot 10^6$	$2.07 \cdot 10^6$	$1.92 \cdot 10^6$
FIN2	$5.98 \cdot 10^6$	$6.33 \cdot 10^6$	$6.72 \cdot 10^6$	$6.72 \cdot 10^6$	$5.88 \cdot 10^6$	$4.87 \cdot 10^6$	$3.42 \cdot 10^6$	$2.56 \cdot 10^6$
FIN3	$5.14 \cdot 10^6$	$5.59 \cdot 10^6$	$5.65 \cdot 10^6$	$5.65 \cdot 10^6$	$4.78 \cdot 10^6$	$4.10 \cdot 10^6$	$4.10 \cdot 10^6$	$3.96 \cdot 10^6$

3.2 Fluid-Structure Interaction calculations results

The calculations were performed until the convergence of forces and displacement of the fin was obtained, and it was reached after about 12 seconds of simulation time. The average time of computations on the 64 GB work station with two Intel Xeon E5-2680 processors was equal to 36 hours.

Figure 8 presents the values of the lift force (on the left) and drag force (on the right) in relation to the angle of attack for the speed equal to 10 m/s and three analysed fins. Figure 9 presents the relation between the angle of attack for fins and tip displacement.

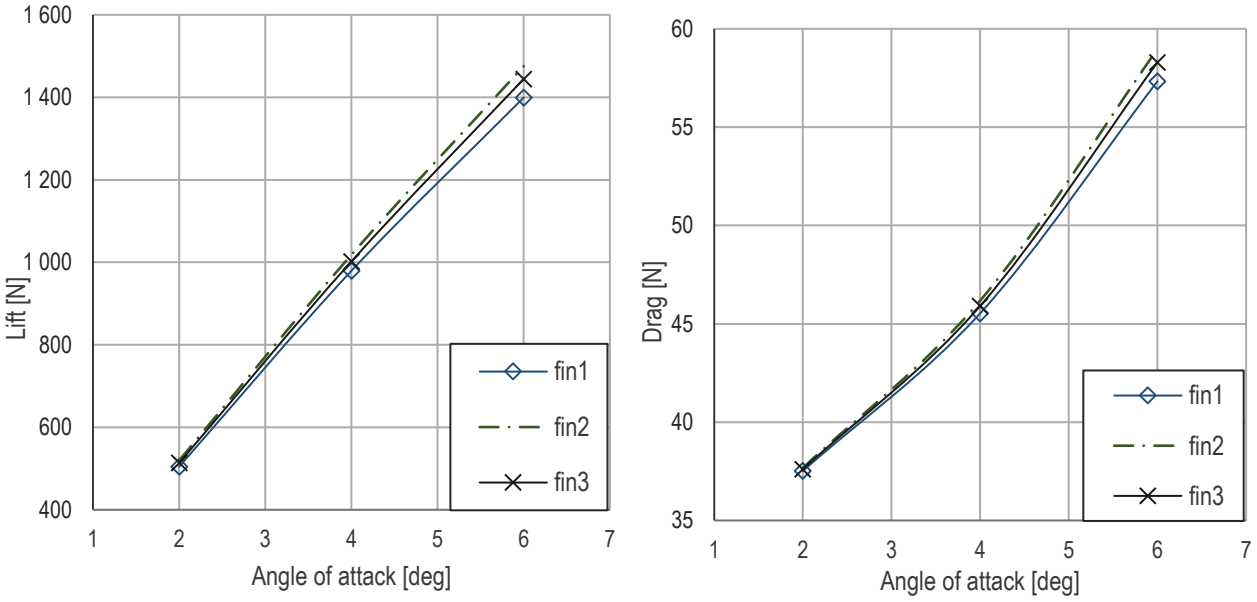

Figure 8. Lift and drag force vs angle of attack

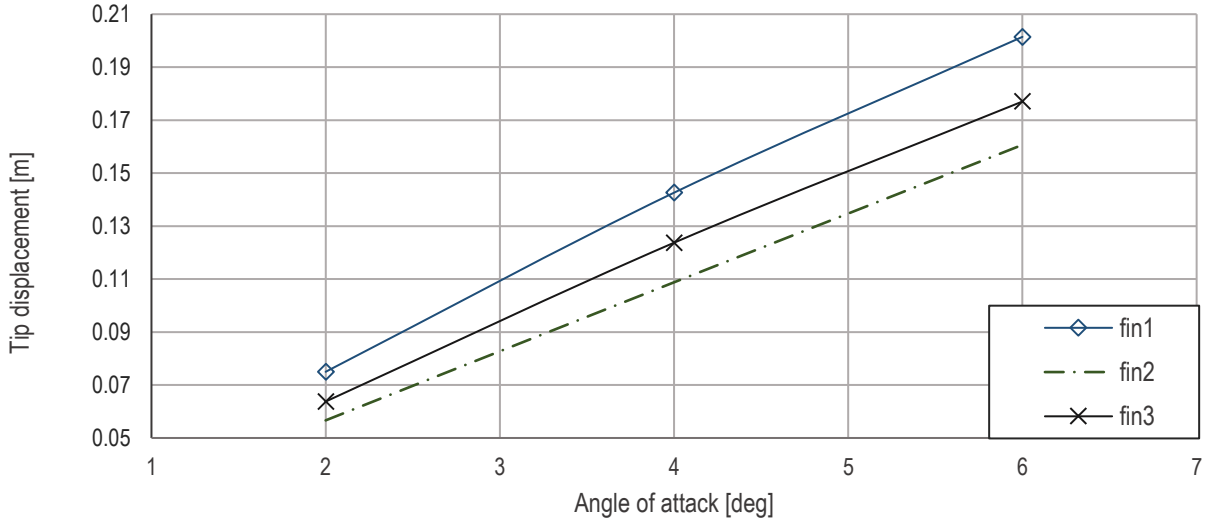

Figure 9. Tip displacement in relation to the angle of attack

The lift force is the dominating force, compared to the buoyancy and drag force, acting on the direction characterised by the smallest cross-section moment of inertia. Therefore, it is the main contributing factor to the resulting deflection of the hydrofoil. The highest bending stiffness had FIN2, which is characterised by the highest values of lift force and drag. It is expected that the difference in the drag force is somehow related to the higher lift. Consequently, higher induced drag could be the reason for the higher total drag rather than local changes in the angle of attack. Significant differences in tip displacement could be observed.

The left plot in Figure 10 presents the relation between the lift force generated by the hydrofoil and the resulting tip displacement. It can be noticed that for the selected composite material model, the linear relation between the lift and displacement for all three fins occurs. The right plot presents the relation between displacement and drag force. For the drag forces the linear relationship does not occur.

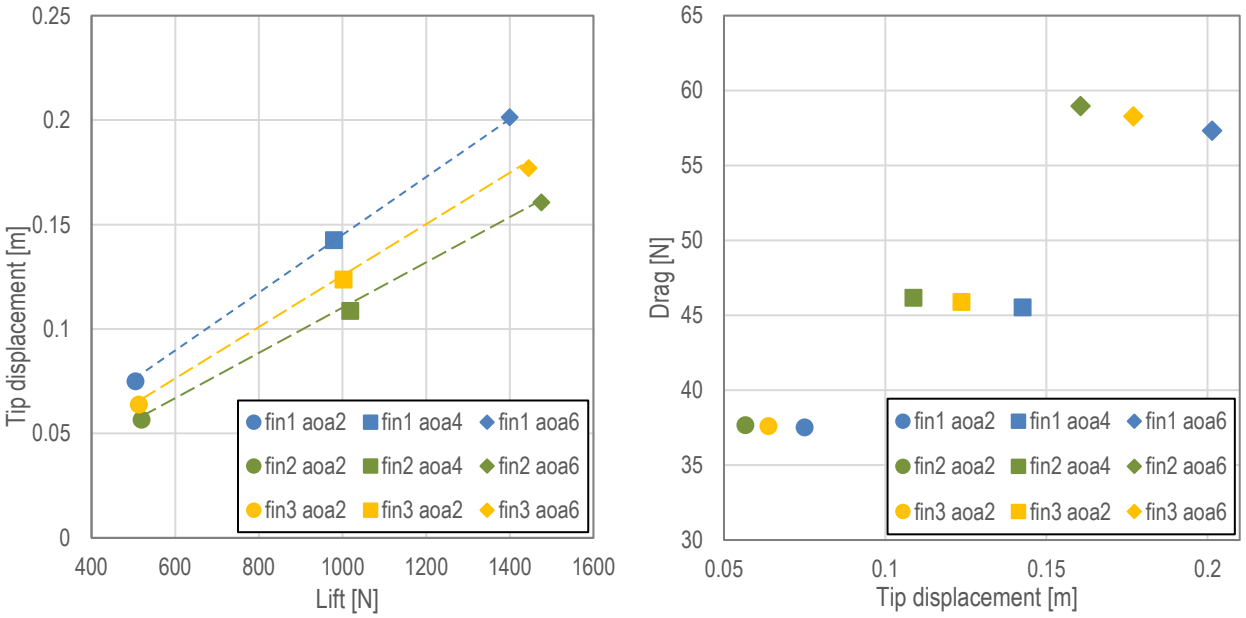

Figure 10. Relation between tip displacement, lift forces and drag forces

Regarding absolute differences, they are smaller for little load acting on the structure and become more significant when higher forces occur. Therefore, in terms of lift generation, the stiffest structure is beneficial; however, it suffers from higher drag.

4. DISCUSSION

The Fluid-Structure Interaction calculations allowed to evaluate the hydroelastic properties of composite fin. According to Figure 8 and Figure 9 the differences between the fins are mainly regarding the structure deformations. The displacement of the most flexible fin is between 32% and 25% higher than for the most stiff fin, and medium fin tip displacement is between 14% and 10% smaller than the most stiff hydrofoil. The relative difference decreased for higher angles of attack.

The difference between the lift force generated by the most flexible and most rigid fin was between 3% and 5%, and between 1% and 2% for medium and rigid fin. Therefore, despite very significant differences in the displacement, the resulting variations in forces are considerably small. The similar situation is with the drag forces, however, here the relative differences between stiff, medium and flexible fin are even smaller and they do not exceed 3% for any case. Comparing the presented values with the one presented by (Pruszko 2021) including the fin stiffness has a major influence of the predicted lift characteristics as the differences between the non-deformable CFD and FSI are in the range from 8 % to 12% for the most flexible fin. The flexibility has little influence on drag.

According to the Figure 10 for the selected range of attacks, the relation between the lift and angle of attack is in the linear region; therefore, the linear reaction between lift and displacement was expected. Therefore, the slope of the curve informs about the stiffness of the fin.

The fin stiffness has a minor influence on the hydrodynamic forces, however, this statement is valid only for the presented case and assumptions. In this study the only variable was plate stiffness expressed as the variations in the Young Modulus of plate sections along the fin span. However, there are several other factors to consider. First of all is the assumption of isotropy and lack of evaluation how the other material constants can influence the hydrodynamic forces.

Second of all, one of the parameters crucial for FSI simulations is the material damping. In this case, it was selected in a way to achieve stable calculations. It was observed that too small material damping is leading to divergence of calculations. On the other hand, material damping has an influence on the convergence simulation time, and high damping increase it. Moreover, it has some influence also on the range of force fluctuations and average value. During this study such problem was observed, however, the influence was not quantified. Another fact that might indicate its importance is the obtained results of the free vibration tests conducted on another group of windsurfing fins presented by (Pruszko and Mikulski 2021). The observed differences in the Eigen-frequencies of windsurfing fin were little, however, the logarithmic damping decrement values were significantly varying. Ideally, for each fin also the damping coefficients should be evaluated and considered in calculations.

Finally, the fins would vary between each other not only in terms of structure stiffness but also geometry. Early stage studies indicates that the influence of geometry can be significant, therefore, the differences in performance is the combined influence of stiffness and geometry. Nevertheless, obtaining detailed information about larger population of fins: 3D scan, structure stiffness distribution and material damping constants seems to be extremely time consuming.

5. CONCLUSIONS

This article addresses the problem of evaluating the hydro-structural properties of the composite windsurfing fin for unknown a-priori exact geometry and composite schedule. Despite the assumption of their identity, everyday practice showed that the fins are different. Variations applies to geometry and structural stiffness which affect performance.

The main objective of the research was quantification of variances in windsurfing stiffness and determination of its influence on the hydromechanical forces, without considering the possible variations in the geometry. The goal of the research was achieved, as the variances in the stiffness distribution and resulting variations in hydrodynamic performance were quantified.

For the assumed simplifications it was found that despite significant differences in structure displacement under the fluid loading (up to 32% between the most rigid and flexible fin) the variations in lift force is much smaller (up to 5%) and variance between the drag forces are almost negligible. Moreover, the linear relation between the lift force and tip displacement for all fins was observed. The important contribution is the method for identifying stiffness distribution for the composite hydrofoil with unknown lay-up.

The presented research has a strong application orientation, as the variances in hydro-structural properties of the composite hydrofoils produced in a series, not as a one-off is quite well known, and this study might be useful from the end-user point of view.

The future works are going to focus on determining and including into numerical model other parameters, such as material damping or other material constants. Moreover, it would be interesting to perform such calculations for the composite modelled as an orthotropic material. Finally the experimental validation of the computations in the towing tank should be performed.

ACKNOWLEDGEMENTS

Calculations were carried out at the Centre of Informatics Tricity Academic Supercomputer & Network

REFERENCES

Balze, Rémy, Nedeleg Bigi, Kostia Roncin, Jean B. Leroux, Alain Nême, Vincent Keryvin, Antoine Connan, Hervé Devaux, and Denis Gléhen. 2017. “An Innovative Tool to Study and Optimize Racing Yacht Appendages Using Fluid-Structure Interactions.” In *7th International Conference on Computational Methods in Marine Engineering, MARINE 2017*, 2017-May:616–24. http://www.gseadesign.com/Webpage:http://www.irdl.frWebpage:http://www.irdl.frWebpage:http://www.irdl.fr.

Boyd, S W, D Flannigan, J Banks, and S R Turnock. 2015. “DESIGN OF COMPOSITE CONTROL SURFACES FOR TAILORED DEFORMATION USING FLUID STRUCTURE INTERACTIONS.” In *LIMAS -2015: International Conference on Light Weight Design of Marine Structures*.

Cardoso de Brito, Miguel, Leigh Stuart Sutherland, José Manuel C. Pereira, and Mário Rui Arruda. 2022. “Fluid-Structure Interaction Analyses for Hydro-Elastic Tailoring of a Windsurfer Fin.” *Journal of Marine Science and Engineering* 10 (10). https://doi.org/10.3390/jmse10101371.

Chróścielewski, Jacek, Tomasz Ferenc, Tomasz Mikulski, Mikołaj Miśkiewicz, and Łukasz Pyrzowski. 2019. “Numerical Modeling and Experimental Validation of Full-Scale Segment to Support Design of Novel GFRP Footbridge.” *Composite Structures* 213. https://doi.org/10.1016/j.compstruct.2019.01.089.

Ferenc, Tomasz, and Tomasz Mikulski. 2020a. “Parametric Optimization of Sandwich Composite Footbridge with U-Shaped Cross-Section.” *Composite Structures* 246. https://doi.org/10.1016/j.compstruct.2020.112406.

———. 2020b. “Validation Process for Computational Model of Full-Scale Segment for Design of Composite Footbridge.” *Polish Maritime Research* 27 (2). https://doi.org/10.2478/pomr-2020-0037.

Giovannetti, Laura Marimon, Ali Farousi, Fabian Ebbesson, Alois Thollot, Alex Shiri, and Arash Eslamdoost. 2022. “Fluid-Structure Interaction of a Foiling Craft.” *Journal of Marine Science and Engineering* 10 (3).

https://doi.org/10.3390/jmse10030372.

ITTC. 2011. “Practical Guidelines for Ship CFD Applications - 7.5-03-02-03.” In *ITTC – Recommended Procedures and Guidelines*, 1–18.

Kreja, Ireneusz, and Agnieszka Sabik. 2019. “Equivalent Single-Layer Models in Deformation Analysis of Laminated Multilayered Plates.” *Acta Mechanica* 230 (8). https://doi.org/10.1007/s00707-019-02434-7.

Marimon Giovannetti, L. 2017. “Fluid Structure Interaction Testing, Modelling and Development of Passive Adaptive Composite Foils.”

Marimon Giovannetti, L., J. Banks, M. Ledri, S. R. Turnock, and S. W. Boyd. 2018. “Toward the Development of a Hydrofoil Tailored to Passively Reduce Its Lift Response to Fluid Load.” *Ocean Engineering* 167 (November): 1–10. https://doi.org/10.1016/j.oceaneng.2018.08.018.

Maung, Phyo Thu, B. Gangadhara Prusty, Md Shamsuddoha, Andrew W. Phillips, and Nigel A. St John. 2021. “Static and Dynamic Response of a Carbon Composite Full-Scale Hydrofoil Manufactured Using Automated Fibre Placement.” *Composites Part C: Open Access* 6: 100218. https://doi.org/10.1016/j.jcomc.2021.100218.

Navagally, Rahul Reddy. 2017. “Composite Materials - History, Types, Fabrication Techniques, Advantages, and Applications.” *International Journal of Mechanical And Production Engineering* 5 (9).

Ponte, R., L. Sutherland, and Y. Garbatov. 2022. “Structural Analysis of a ‘Foiling Moth’ Sailing Dinghy Hydrofoil.” In *Trends in Maritime Technology and Engineering Volume 1*, 185–91. CRC Press. https://doi.org/10.1201/9781003320272-21.

Pruszko, Hanna. 2021. “Mesh Dependence Study for Numerical Assessment of Hydrodynamic Characteristics of Windsurfing Fin.” In *Hydronav - International Symposium on Hydrodynamics in Ship Design, Safety, Manoeuvring and Operation*, 66–71. https://oio.pg.edu.pl/documents/102415222/104817833/E-book_Hydronav2021.pdf.

Pruszko, Hanna, and Tomasz Mikulski. 2021. “ACCELEROMETRIC MEASUREMENTS OF WINDSURFING FINS VIBRATIONS.” In *International Conference on Postgraduate Research in Maritime Technology 2021*.

Sacher, Matthieu, Mathieu Durand, Élisa Berrini, Frédéric Hauville, Régis Duvigneau, Olivier Le Maître, and Jacques André Astolfi. 2018. “Flexible Hydrofoil Optimization for the 35th America’s Cup with Constrained EGO Method.” *Ocean Engineering* 157 (March): 62–72. https://doi.org/10.1016/j.oceaneng.2018.03.047.

Sacher, Matthieu, Jean Baptiste Leroux, Alain Nême, and Christian Jochum. 2020. “A Fast and Robust Approach to Compute Nonlinear Fluid-Structure Interactions on Yacht Sails – Application to a Semi-Rigid Composite Mainsail.” *Ocean Engineering* 201 (October). https://doi.org/10.1016/j.oceaneng.2020.107139.

Sutherland, L.S., M. Cardoso de Brito, J. Chaves Pereira, M.R. Arruda, and S. Benson. 2022. “Fluid-Structure Interaction Analyses of a Composite Windsurf Fin.” In *Trends in Maritime Technology and Engineering Volume 1*, 223–31. CRC Press. https://doi.org/10.1201/9781003320272-25.